Desalination and Water Treatment
www.deswater.com

49 (2012) 359–367
November

1944-3994/1944-3986 © 2012 Desalination Publications. All rights reserved
doi: 10.1080/19443994.2012.719465

Taylor & Francis
Taylor & Francis Group

Arsenic(III) removal from low-arsenic water by adsorption with amorphous mesoporous TiO_2

Yu-Chao Tang[a,b,*], Chang-Nian Wu[a,b,*], Xian-Huai Huang[a], Hai-Ping Zhang[a,c], Han-Qing Yu[b], Xin Li[a], Yan Peng[a]

[a]*Department of Environmental Engineering, Anhui University of Architecture, Hefei 230022, P.R. China*
Tel. +86 551 3828122; Fax: +86 551 3828223; email: tangyc@aiai.edu.cn
[b]*School of Chemistry and Materials Science, University of Science and Technology of China, Hefei 230026, P.R. China*
Email: cnwu@aiai.edu.cn
[c]*Shenzhen Graduate School, Harbin Institute of Technology, Shenzhen 518055, P.R. China*

Received 22 September 2011; Accepted 19 July 2012

ABSTRACT

The present study investigated the removal of As(III) from low-arsenic water through adsorption on amorphous mesoporous TiO_2. The mesoporous TiO_2 adsorbent size was 3.92 nm as calculated by adsorption average pore width. The Brunauer–Emmett–Teller surface area was 205 m^2/g. A 0.2 g adsorbent treatment during five hours resulted in less than 4 μg/L remaining As(III) in the water, and nearly 84% of As(III) in the solution were removed in only 20 min. The As(III) adsorption kinetics data were well described by the pseudo-second-order model. The maximum adsorption pH value of 9.3 coincided with the first pK_1 dissociation constant of H_3AsO_3 of 9.22. The Dubinin-Radushkevich and Langmuir isotherms provided maximum adsorption capacity of 4.57 and 4.79 mg/g, respectively, under low equilibrium concentration. These values possibly indicate the excellent capacity of amorphous mesoporous TiO_2 on As(III) removal from low-arsenic water. Given by the b-value of Langmuir isotherm under different pH, the average standard Gibbs free energy changes (ΔG^o) was –11.6 kJ mol^{-1}, which indicated spontaneous adsorption.

Keywords: As(III); Adsorption; Amorphous TiO_2; Drinking water treatment

1. Introduction

Groundwater is ubiquitously used for drinking water supply in the world and usually its quality is superior to that of the surface water, for it is typically free from micro-organisms, colloids, and organisms. The elevated concentrations of arsenic in the environment occur from both natural geological backgroundings and anthropogenic sources. Millions of people are at serious risk of arsenic poisoning in many countries around the world, especially in India, Bangladesh, Vietnam, China, and Chile [1]. Arsenic is a highly toxic and carcinogenic element, prompting the World Health Organization (WHO), United States Environmental Protection Agency (USEPA), as well as several countries to lower the maximum contaminant level (MCL) for arsenic in drinking water from 50 to 10 μg/L. In 2003, the state of New Jersey, USA proposed to further lower the MCL to 5 μg/L for assurance of public health [2]. The distribution between As(III) and As(V) in water depends on oxidative and reductive conditions and pH. As(III) predominate in moderately reducing anaerobic environments, such as groundwater, particularly existing as H_3AsO_3 in natural groundwater with a pH value ranging from

*Corresponding author.

weakly acidic to weakly alkaline (pH 6–8). However, literature reported ratios of As(III)/As(total) in groundwater in the range of 0.6–0.9 [3], which is of great concern because As(III) is more toxic than As (V). Under groundwater conditions, As(III) is the predominate form of arsenic, which is more toxic (25–60times) and mobile than As(V) [4].

Several treatment techniques have been developed to remove arsenic from drinking water, namely, electrocoagulation [5], adsorption [6,7], coagulation [8], nanofiltration [9–11], dialysis and reverse osmosis [12], as well as ion exchange [13]. Adsorption is believed to be the simplest, most efficient, and cost effective among these techniques, especially for low arsenic concentration such as that in natural surface water or groundwater [14]. Mohan and Pittman [15] reviewed various adsorbents for arsenic removal from drinking water or wastewater. The nonionic existence of As(III) in natural water makes it generally reported to have lower affinity to the surface of various adsorbents compared with As(V) [16]. Thus, a pretreatment of As(III) through oxidation to As(V) and/or adjusting the water pH value before treatment may be necessary. Concentrations of As(III) and As(V) in contaminated groundwater in general are relatively low, thus, the adsorption property of an adsorbent in the range of low arsenic concentration may be a highly critical factor affecting its application in drinking water supply.

Recently, titanium dioxide (TiO_2) has attracted significant research interest and has been considered as a promising arsenic adsorbent for its nontoxicity, commercial availability, high stability, and high adsorption potential [16–19]. The TiO_2 has been reported to effectively remove As(III) from water even without the preoxidation process [20–23]. Xu et al. [18] reported nanoparticle TiO_2 prepared through hydrolysis of aqueous $TiCl_4$ solution; its adsorption capacity for As (III) reached over 83 mg/g at nearly neutral pH environment. TiO_2 reached its maximum adsorption capacity for As(III) at about pH 9, a value relatively close to that of alkalescent groundwater environments, suggesting that TiO_2 is favorable for adsorbing As(III) in natural weakly alkaline groundwater. Pena et al. [1] reported surface complexes formed between TiO_2 and arsenic species, and maintained the nonprotonated speciation at pH values of 5–10. They found the dominant surface species to be $(TiO)_2$-AsO_2^- and $(TiO)_2$-AsO^- for As(V) and As(III), respectively. The potential of TiO_2 for arsenic removal has thus been proven. Macroscopic investigations on metal adsorption showed that higher surface areas cause amorphous metal oxides to have larger adsorption capacities compared with their crystalline morphology [24]. However, limited studies have focused on adsorption behaviors and mechanisms of As(III) on amorphous TiO_2. Jegadeesan et al. [25] and Manna et al. [26] found amorphous TiO_2 to have a disordered surface structure, small particle size, and high-surface area that increases its effectiveness as adsorbent for arsenic removal.

Therefore, the main objectives of the present work are: (1) to prepare an amorphous mesoporous TiO_2 adsorbent through simple hydrolysis from environmentally friendly and low-cost raw materials for effective arsenic removal; (2) to characterize the adsorbent with a variety of techniques; and (3) to evaluate its As (III) adsorption capacities and performances, i.e. equilibrium, kinetics aspects, and effects of pH.

2. Experimental

2.1. Chemicals and materials

Amorphous mesoporous TiO_2 was prepared by hydrolysis process. Liquid tetrabutyl titanate ($Ti(OC_4H_9)_4$, 99.0%, Sinopharm Chemical Reagent Co. Ltd, Shanghai) and arsenic(III) oxide (As_2O_3, Jingchun Chemical Reagent Co. Ltd, Shanghai) were employed as the raw material for amorphous TiO_2 and stock solutions for As(III), respectively. Concentrated hydrochloride acid (HCl, 32–38%, Sinopharm Chemical Reagent Co. Ltd, Shanghai) and sodium hydroxide (NaOH, Sinopharm Chemical Reagent Co. Ltd, Shanghai) were used to fix pH and thus arsenic speciation.

2.2. Amorphous mesoporous TiO_2 preparation

The amorphous mesoporous TiO_2 was prepared according to [27]. 20 mL of acetic acid was mixed with 40 mL ($Ti(OC_4H_9)_4$). In order to hydrolyze it, 50 mL aqueous ammonia (30%) and deionized water was added dropwise to the mixture with a rate of 1 mL/min until the pH reach 9. The hydrolysis of tetrabutyl titanate was operated on an electric jacket (JB-90-2, shanghai balance Instrument Co. Ltd) at 1,500 rpm and solution temperature controlled at 20 ± 2°C. The hydrolysis product was stirred continuously during 60 min. The precipitate (hydrolysis product) obtained was white and then rinsed with 500 mL deionized water several times during about 1 h. The precipitate was then dried at 60°C for 24 h under air. Then, the dried precipitate was crushed into fine powders in agate mortar to obtain the desired amorphous mesoporous TiO_2 particles.

2.3. Amorphous mesoporous TiO_2 characterization

X-ray diffraction (XRD) patterns were obtained using diffraction spectroscopy with Ni filter and

graphite monochromator (D/max-rA, Rigaku Corporation, Japan) at room temperatures. The X-ray source was from Cu K_a radiation ($\lambda = 1.54187$ Å) and 2θ ranged from 20° to 80°. Brunauer–Emmett–Teller (BET) surface area was examined by N_2 adsorption–desorption isotherm with a TriStar II 3020M series surface area and pore size analyzers (TriStar II 3020M, Micromeritics Instrument Corporation, USA). The analysis bath temperature was –195.850°C. The morphology of the powder was observed by transmission electron microscopy (TEM) and carried out on a JEOL 2010 TEM (JEOL Ltd, Japan), operating at 200 kV, with point-to-point resolution of 0.194 nm. TEM samples were made by scattering the powder with diluted ethyl alcohol under ultrasonic wave and then dispersing it on a Cu grid.

2.4. Arsenic adsorption experiments

The adsorption kinetics, isotherms, and behavior of the adsorbent for As(III) removal were investigated. Arsenic contaminated water was realized by dilution a given amount of As(III) stoke solution by tap drinking water (see Table 1). To study adsorption rates and kinetics, batch experiments were carried out by adding various concentrations of amorphous mesoporous TiO_2 (0.1, 0.2, and 0.3 g/L) into 1,000 mL water with initial As(III) concentrations of 150 μg/L at a temperature of 25°C. Similar experiments were realized by adding various concentration of As(III) (80, 150, and 500 μg/L) into 1,000 mL water with 0.2 g/L adsorbent at the same temperature. The pH value of the solutions was adjusted with HCl and NaOH to reach values of about 3–12, measured by a pH meter (FE20, Mettler Toledo Instrument Co., Ltd, Switzerland). Before adding the adsorbent, As(III) solution was heated to fix temperature. The temperatures were controlled in a sealed homoeothermic incubator, stirring at 60 rpm. At the given reaction intervals, 3 mL aliquots were sampled and immediately filtered through 0.45 μm filter film (Millipore Corporation, USA). Agglomeration of these nanoparticles was observed in aqueous solutions (bulk particle size >1.0 μm), and therefore the adsorbents were unlikely to pass through 0.45 μm filters.

Adsorption isotherms were obtained from the experiments by adding different amounts of adsorbents into 100 mL As(III) solutions with concentration of 250 μg/L. The pH value was adjusted to about 5.0, 7.0, and 9.0 by adding HCl and NaOH at temperature of 25°C. After 24 h of mixing, the samples were filtered through 0.45 μm filter film. Variations in the concentration of As(III) were monitored by atomic absorption spectrophotometer (AAS, TAS-990, Beijing Puxi Instrument Co., Ltd, China). A hydride generation system was connected to the equipment and the arsine was atomized in a quartz cell [28]. The detection limit was 0.25 μg/L.

Table 1
Characterization of tap drinking water used for experiment

Components	Concentrations (mg/L)
pH	7.1–7.4
Chloride	11–25
Iron	0.024
Sodium	6–17
Sulfate	14–22

3. Results and discussion

3.1. Surface properties and morphology of amorphous mesoporous TiO_2 adsorbent

Fig. 1(a) shows the BET measurement curves of amorphous mesoporous TiO_2 particles. These nanoparticles had a pore size distribution derived from adsorption data using the Barrett–Joyner–Halenda (BJH) model (Fig. 1(b)). The sample BET specific surface area was calculated to be 205 m^2/g. Measured at $P/P_0 = 0.972$, the total volume of pores less than 71.4 nm diameter was 0.201 cm^3/g.

The BET curve calculations produced the shape and size characteristics of cylindrical pores and mesopores, suggesting limited micropores in the test particles [20]. Calculated by adsorption average pore width (4 V/A by BET), the test particles had pore size of 3.92 nm, which fall within the range of mesoporous dimension and suitable for use as adsorbent. The BJH adsorption cumulative surface area of pores within 1.7–300 nm in diameter was 221 m^2/g. About 90% (199 m^2/g) of the surface area might come from nanoparticles with pore diameter ranging from 1.9 to 6.0 nm (coinciding with the BET curve shape, as shown in Fig. 1(b), by which the mesoporous structure was verified). Thus, these amorphous mesoporous TiO_2 adsorbent created through hydrolysis had relatively large specific surface areas and huge pore volumes, which contribute to its excellent adsorption potential.

The XRD patterns of mesoporous TiO_2 (data not shown) showed no distinct peaks at 2θ ranging from 20° to 80°, suggesting an amorphous adsorbent obtained through hydrolysis. TEM images of amorphous mesoporous TiO_2 (Fig. 1(c)) indicate nanosized

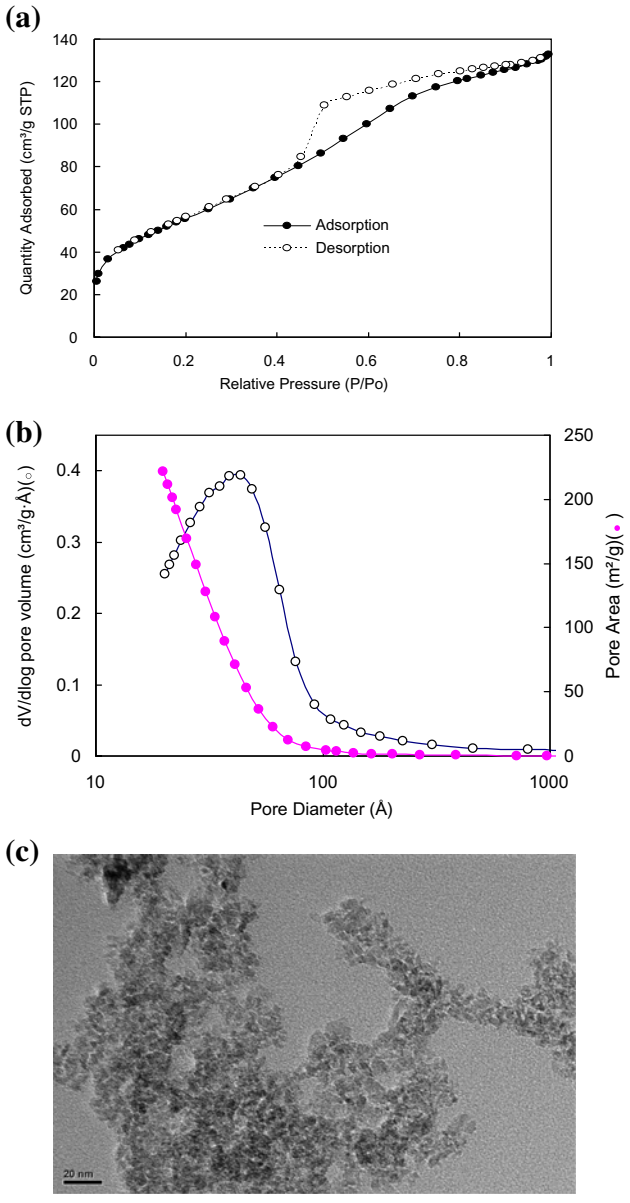

Fig. 1. (a) BET curve, (b) BJH adsorption dV/dlog(D) pore volume and cumulative pore area, and (c) TEM micrograph of amorphous mesoporous TiO_2 particles.

particles with rubble shapes. The average particle size is about 1–3 μm. Aggregating into micrometer-sized particles was observed by the TEM. The formation of nonuniform micrometer-sized particles through this aggregation process leads to a mesoporous particle structure. This aggregation benefited the removal of resultant micrometer-sized particles from drinking water through sedimentation. The important physical and surface properties of TiO_2 adsorbent are presented in Table 2.

Table 2
Physical and surface properties of TiO_2 adsorbent

Properties	Quantitative value
BET	205 m^2/g
Crystal	Amorphous
Pore size	3.92 nm
Pore volume	0.201 cm^3/g

3.2. Kinetic studies on As(III) adsorption by amorphous mesoporous TiO_2

Treated with 0.2 g/L amorphous mesoporous TiO_2 adsorbent dosage, less than 4 μg/L of As(III) remained in the solution (initial concentration 150 μg/L), suggesting efficient removal. Moreover, most of the As (III) was adsorbed in a very short time. For example, a 0.30 g/L dosage of amorphous mesoporous TiO_2 removed nearly 84% of As(III) in the solution in only 20 min. The initial high adsorption rate is beneficial to engineering applications for cost-effective water treatment.

The adsorption process is considered heterogeneous, and thus the adsorption rate depends on the solution concentration and active sites on TiO_2 [29]. In the case of strict surface adsorption process, a rate variation should be proportional to the first power of concentration [30]. Initially, the adsorption rate showed a nearly linear correlation of the dissolved As (III) concentration in the solutions; therefore, the first-order reaction model or pseudo-first-order reaction model might be applied to describe adsorption kinetics in this stage. Approaching the adsorption equilibrium state, the apparent adsorption rate decreased to almost 0 regardless of the residual As(III) concentration in the solution. Based on the former discussion, the kinetics of the entire heterogeneous adsorption process can be described by the first-order reaction model or pseudo-first-order reaction model [3,31], pseudo-second-order model [3,20,21], Elovich kinetic equation [21,32], and power function kinetic model, among others [29,33].

In the present study, the As(III) adsorption kinetics data were found to match the pseudo-second order model (Fig. 2), which can be described by the equation [20,21]:

$$\frac{t}{Q_t} = \frac{1}{K_2 \cdot Q_e^2} + \frac{t}{Q_e} \quad (1)$$

in which Q_t and Q_e (mg/g) are As(III) amounts adsorbed at time t and at equilibrium, respectively; and K_2 is constant rate. Thus, when the initial

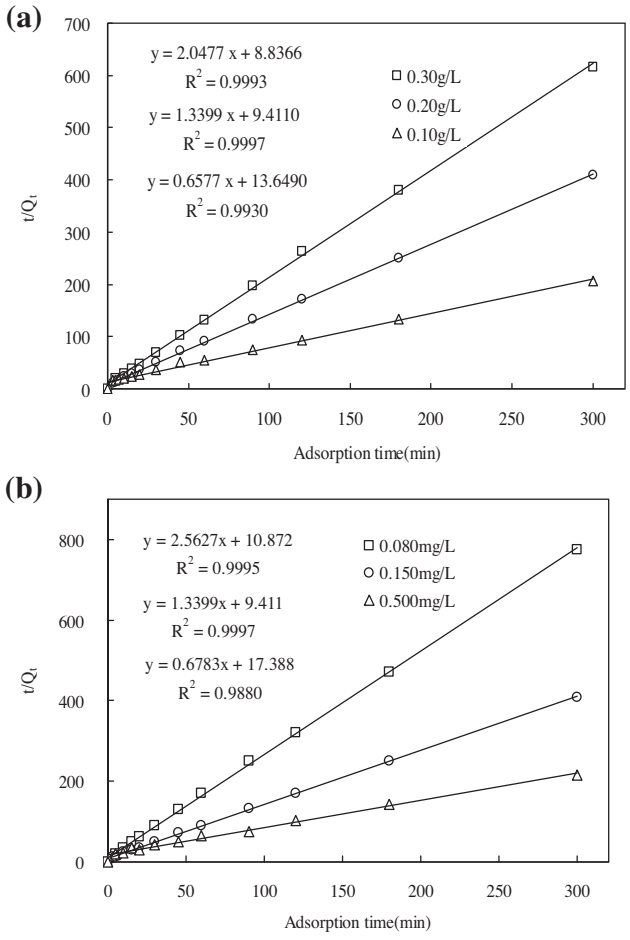

Fig. 2. A plot of As(III) adsorption data using the pseudo-second-order model at (a) various adsorbent dosage (0.10, 0.20, and 0.30 g/L) and (b) various initial As concentrations (80, 150, and 500 μg/L).

concentration of As(III) was 150 μg/L, Q_e was 1.51, 0.746, and 0.488 mg/g of adsorbent dosages of 0.1, 0.2, and 0.3 g/L, respectively.

The reaction kinetics data could not highlight the rate-limiting step in the adsorption process. The rate-limiting step may be either the liquid–solid boundary layer (film control) or the intraparticle diffusion (pore control) of solute on the solid surface from the solution in a batch process [3]. Apart from the adsorption on the adsorbent outer surface, adsorptive ions may move from the solution to the adsorbent pores due to stirring in the batch process.

The functional relation (Eq. (2)) frequently used to predict the rate-limiting step of the adsorption reactions is represented by Eq. (2) [34–37]:

$$Q_t = kt^{0.5} \quad (2)$$

in which k is the intraparticle diffusion rate constant ($mg\,g^{-1}\,t^{-0.5}$) of the reaction. If the rate-controlling step is the pore diffusion, the plot of Q_t against the square root of time should be a straight line passing through the origin. Fig. 3 shows the plots of Q_t vs. $t^{0.5}$ for As(III) adsorption. The nonlinear plots that do not pass through the origin indicate that the present adsorption reactions rates may not be controlled by pore diffusion but by the boundary layer (film) diffusion.

3.3. Effect of pH on As(III) adsorption by amorphous mesoporous TiO_2

Fig. 4 shows the effect of pH on As(III) adsorption on amorphous mesoporous TiO_2, and the constant rate k of the pseudo-second-order reaction model as a function of equilibrium pH. The constant rate k of As (III) removal increased from 0.018 to 0.027 $L\,mg^{-1}$ min when pH increased from 3.04 to 9.3. However, k dramatically decreased to 0.0101 $L\,mg^{-1}$ min when pH increased from 9.3 to 12.11. The maximum adsorption capacity of As(III) approximately occurred at pH 9.3, coinciding with pK_1 9.22, which is the first dissociation constant of H_3AsO_3. Similar adsorption behaviors of As(III) on nanocrystalline TiO_2 were previously reported [1,22].

Previous studies reported that in an acid pH environment, the neutrality of As(III) species (in the H_3AsO_3 form) would inhibit the adsorption or precipitation of As(III) from solutions [38,39]. Bang et al. [22], Dutta et al. [29], and Yang et al. [40] reported that the adsorption of As(V) under acidic conditions was

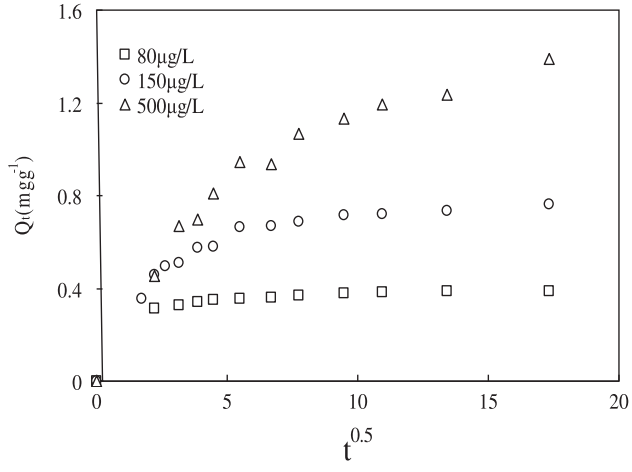

Fig. 3. The Weber-Morris plots for intraparticle diffusion of the As(III) adsorption kinetic data on amorphous mesoporous TiO_2 (adsorbent dosage = 0.2 g/L; initial As (III) concentrations: 80, 150, and 500 μg/L; and pH 7.17).

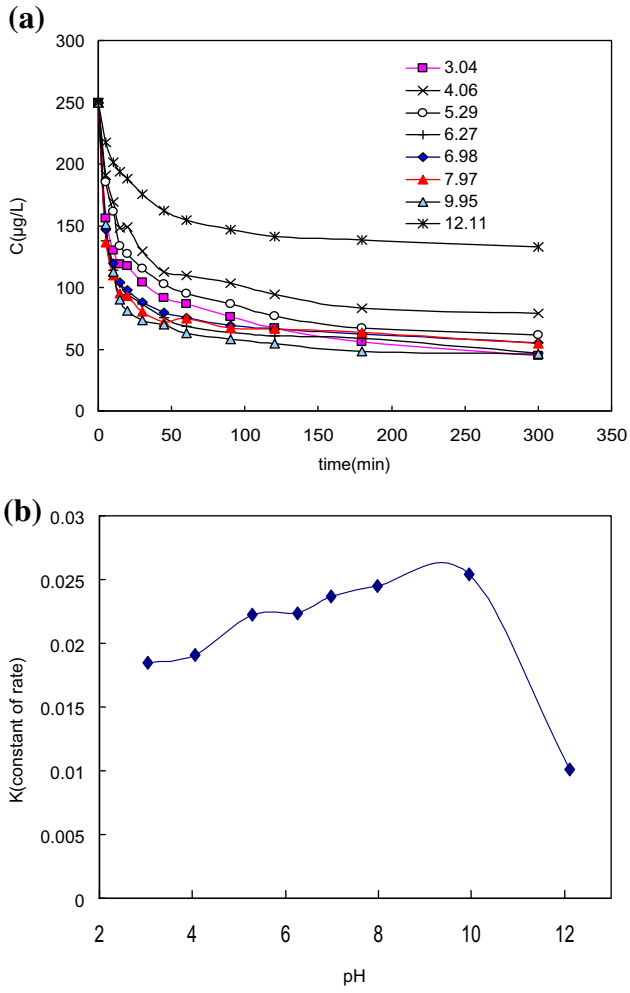

Fig. 4. Effect of pH on As(III) adsorption by amorphous mesoporous TiO_2 (a) concentration as a function of time, (b) constant rate k as a function of equilibrium pH (initial As concentration = 250 μg/L; contact time = 5 h; and adsorbent dosage = 0.20 g/L).

stronger than at pH 9. They explained this adsorption by electrostatic considerations. The predominant As (V) species exist as $H_2AsO_4^-$ and $HAsO_4^{2-}$ in the pH range of 2.2–11.5. Otherwise, As(III) exists predominantly in the H_3AsO_3 form for pH < 9.2 and as $H_2AsO_3^-$ for pH > 9.2. This may indicate electrostatic considerations was not the main As(III) adsorption pattern.

In the present study, efficient removal of As(III) in near neutral solution, varying from weak acid to weak alkaline environments, proved that nonionic H_3AsO_3 in near neutral water does not prevent the contact of As(III) with TiO_2 in the adsorption process. Thus, a strong binding force may have formed between nonionic H_3AsO_3 and amorphous mesoporous TiO_2 during adsorption. Otherwise, the decreasing As(III) removal rate, along with increasing pH, was attributed to the decreasing number of positively charged active sites on particle surfaces and the increasing OH^- ions in solution. OH^- ions in solution will compete with $H_2AsO_3^-$ for adsorption on the hydroxide titanium surface. Jing et al. [1] demonstrated that the As(V) and As(III) species formed negatively charged inner-sphere surface complexes as the value of the TiO_2 point of zero charge (PZC) decreased from 5.8 to 5.2 after the adsorption reactions. The strong adsorption behaviors of As(III) at the value of pH > PZC indicated that the arsenic species were adsorbed onto amorphous mesoporous TiO_2 through the surface complex rather than by electrostatic interactions [22].

3.4. Equilibrium adsorption isotherm of As(III) by amorphous TiO_2

The Langmuir isotherm model assumes a monolayer surface coverage limiting the adsorption due to surface saturation, whereas the empirical Freundlich isotherm model allows the multilayer adsorption [41]. The Langmuir adsorption isotherm can be expressed as:

$$Q_e = \frac{Q_m(b \cdot C_e)^n}{[1 + (b \cdot C_e)^n]^{\frac{m}{n}}}, \quad (3)$$

where Q_e (mg/g) is the specific adsorbed quantity of a model pollutant compound with a concentration C_e (mg/L), at equilibrium state; Q_m (mg/g) is the saturation (maximum) adsorption capacity and b is the ratio of K_a/K_d; K_a and K_d are the adsorption and desorption constants; and m and n are irregular particle constants. Unique adsorption sites, monolayer adsorption, and no interaction between adsorption sites are the underlying assumptions used in derived the Langmuir isotherm equation.

The Freundlich adsorption isotherm equation can be expressed as

$$Q_e = K_f C_e^{\frac{1}{n}}, \quad (4)$$

where K_f and n are two Freundlich isotherm parameters. The Freundlich isotherm fits As(III) whatever pH value, which may indicate surface heterogeneity due to the involvement of both strong and weaker binding sites for adsorption. Thus, a multisite adsorption process occurs for these adsorbed ions [29].

Experimental data fit the above two models when the C_e of As(III) is within 10–220 μg/L (Fig. 5(a)). A least square regression analysis produced correlation coefficients (R^2) of 0.952, 0.986, and 0.978 for the Lang-

muir isotherm, and 0.935, 0.990, and 0.995 for the Freundlich isotherm, corresponding to the pH values at 5.04, 7.14, and 9.03, respectively. If $C_e > 220\ \mu g/L$, then

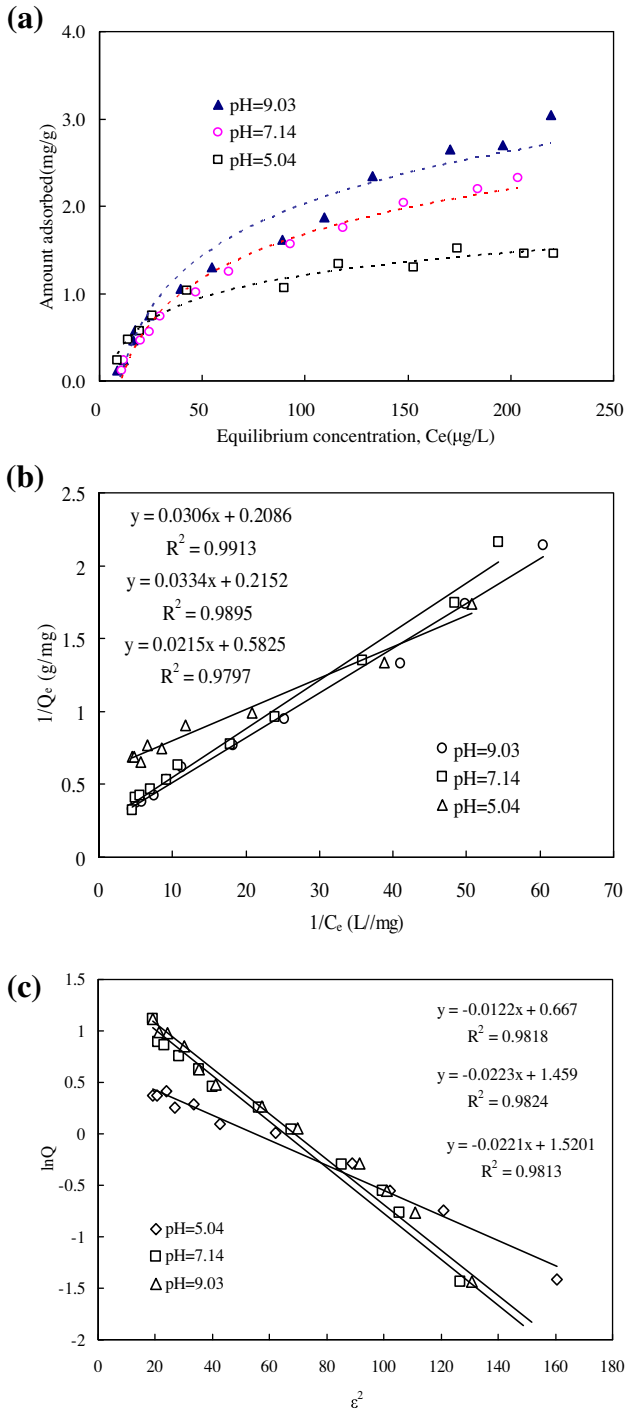

Fig. 5. (a) Equilibrium adsorption capacity, (b) Langmuir isotherm model, and (c) D–R isotherm model of As(III) adsorbed by amorphous mesoporous TiO_2 (initial As concentration = 250 μg/L; contact time = 24 h; and adsorbent dosage in range 0.05–10.0 g/L).

Q_e would significantly exceed the trend extrapolation by Langmuir or Freundlich isotherms. Thus, different driving forces of As(III) adsorption on amorphous TiO_2 nanoparticles are suggested to dominate under lower or higher concentration of As(III) solution. Adsorption capacity and b were calculated from the intercept and slope of the Langmuir isotherm graphs at low equilibrium concentrations (Fig. 5(b)), producing 1.72 mg/g and 0.0271 at pH = 5.04, 4.65 mg/g and 0.00645 at pH = 7.14, as well as 4.79 mg/g and 0.00681 at pH = 9.03, respectively (Table 3).

Langmuir and Freundlich isotherm models cannot interpret the adsorption mechanism. In the present study, the Dubinin–Radushkevich (D–R) isotherm model was applied to obtain better understanding of the adsorption mechanisms [36,42]. The D–R isotherm model can be expressed as the following equations:

$$\ln Q = \ln Q_m - k\varepsilon^2, \tag{5}$$

in which ε (Polanyi potential) can be expressed as:

$$\varepsilon = RT \ln[(1 + (1/C_e)] \tag{6}$$

The Q is the amount of arsenic adsorbed at equilibrium per unit weight of adsorbent (mg/g); Q_m is the maximum adsorption capacity (mg/g); C_e is the arsenic equilibrium concentration in the solution (ppm); k is the constant related to adsorption energy ($mol^2\,kJ^{-2}$); R is the gas constant ($kJ\,mol^{-1}\,K^{-1}$); and T is the temperature (K). Plotting ln Q against ε^2 illustrated the D–R isotherm (Fig. 5(c)). Q_m and k were calculated from the graph slope and intercept as 1.95 mg/g and $-0.0122\ mol^2\,kJ^{-2}$ of pH = 5.04, 4.30 mg/g and $-0.0223\ mol^2\,kJ^{-2}$ of pH = 7.14, as well as 4.57 mg/g and $-0.0221\ mol^2\,kJ^{-2}$ of pH = 9.03, respectively, where k was independent of T. The calculated maximum adsorption capacity at low equilibrium concentrations were approximately equal to those calculated using the Langmuir isotherm of each pH (Table 2). The maximum adsorption capacity of 4.65 mg/g (Langmuir isotherm) and relatively high

Table 3
Maximum adsorption capacities calculated by the Langmuir isotherm and the D–R isotherm

pH	Adsorption capacities(mg/g)	
	Langmuir	D–R
5.04	1.72	1.95
7.14	4.65	4.30
9.03	4.79	4.57

equilibrium adsorption capacities at 1.51 mg/g may indicate the excellent capacity of amorphous mesoporous TiO_2 in As(III) adsorption at low concentration. Lower adsorption capacities were reported by Thirunavukkarasu et al. [43] with maximum adsorption capacity of As(III) adsorbed on iron oxide coated sand (IOCS) at 0.136 mg/g under concentration of 100 μg/L. Singh and Pant [36] reported a maximum adsorption capacity of 0.180 mg/g adsorbed on activated alumina under concentration of 1,000 μg/L. Hsu et al. [44] reported maximum adsorption capacity of 0.0115 mg/g when As(III) adsorbed on reclaimed IOCS with initial concentration at 300 μg/L. Rahaman et al. [45] found that at initial concentration of 333 μg/L, the equation adsorption capacities of As(III) on the fish scale can be calculated by the equation $X = 0.6847C_e^{0.6113}$, and maximum adsorption capacity was 24.75 μg/g calculated using Langmuir isotherm.

Furthermore, the standard Gibbs free energy changes (ΔG°) for the adsorption process can be obtained through the following equation:

$$\ln\left(\frac{1}{b}\right) = \frac{\Delta G^\circ}{RT}, \tag{7}$$

in which b is the Langmuir isotherm constant; R is the universal gas constant (8.3145 J mol^{-1} K^{-1}); and T is the absolute temperature (K). The calculated ΔG° values in the current study were −9.24, −12.9, and −12.8 kJ mol^{-1}, corresponding to pH values of 5.04, 7.14, and 9.03, respectively. The negative ΔG° values indicated spontaneous adsorption. Nabi et al. [23], Maji et al. [37], and Kanel et al. [46], reported similar findings on As(III) removal on the surface of titanium dioxide, laterite soil, and nanoscale zero-valent iron, respectively.

4. Conclusions

Amorphous mesoporous TiO_2 was prepared through the hydrolysis process of tetrabutyl titanate. The mesoporous TiO_2 was characterized by a relatively large surface area and moderate pore volume, demonstrating an excellent capacity for adsorption. The amorphous mesoporous TiO_2 efficiently removed As(III) from low-arsenic water even without a preoxidation process. With TiO_2 0.2 g/L, less than 4 μg/L (lower than the most rigid MCL of arsenic in drinking water) of the initial 150 μg/L concentration of As(III) remained in the solution. The As(III) adsorption kinetics data fit the description of the pseudo-second-order model. The rate-limiting step of the As(III) adsorption on the amorphous mesoporous TiO_2 was regulated by the liquid–solid boundary film control process. The high initial adsorption rate would be beneficial to engineering applications for its low cost. Maximum adsorption capacities calculated using the D–R isotherm at low equilibrium concentrations were approximately the values obtained using the Langmuir isotherm. These maximum adsorption capacities and equation adsorption capacities calculated with the kinetics model under certain conditions suggest the excellent capacity of amorphous mesoporous TiO_2 for As(III) adsorption at low concentration. Such adsorption might be one of the most promising treatments of low concentration As(III) contaminated drinking water.

Acknowledgments

This work was supported by the Natural Science Foundation of China (NSFC, No. 50908001, 51078001), Key Special Program on the S&T for the Pollution Control and Treatment of Water Bodies (No. 2008ZX07316, 2008ZX07103), Special Science and Technology Foundation of Anhui Province (No. 08010301106), International Corporation Project of Science and Technology of Anhui Province (No. 09080703035), and the Anhui Natural Science and Technology Foundation (Excellent Youth Foundation, No. 10040606Y29).

References

[1] M. Pena, X.G. Meng, G. Korfiatis, C.Y. Jing, Adsorption mechanism of arsenic on nanocrystalline titanium dioxide, Environ. Sci. Technol. 40 (2006) 1257–1262.
[2] C. Christen, New Jersey proposes toughest arsenic standard worldwide, Environ. Sci. Technol. 3(8) (2004) 105A.
[3] K. Gupta, U.C. Ghosh, Arsenic removal using hydrous nanostructure iron(III)–titanium(IV) binary mixed oxide from aqueous solution, J. Hazard. Mater. 161 (2009) 884–892.
[4] T.B. Mlilo, L.R. Brunson, D.A. Sabatini, Arsenic and fluoride removal using simple materials, J. Environ. Eng. 136 (2010) 391–398.
[5] M. Kobya, F. Ulu, U. Gebologlu, E. Demirbas, M.S. Oncel, Treatment of potable water containing low concentration of arsenic with electrocoagulation: Different connection modes and Fe–Al electrodes, Sep. Purif. Technol. 77 (2011) 283–293.
[6] H.C. Kim, C.G. Lee, J.A. Park, S.B. Kim, Arsenic removal from water using iron-impregnated granular activated carbon in the presence of bacteria, J. Environ. Sci. Heal. A. 45 (2010) 177–182.
[7] L. Yan, H. Yin, S. Zhang, F. Leng, W. Nan, H. Li, Biosorption of inorganic and organic arsenic from aqueous solution by *Acidithiobacillus ferrooxidans* BY-3, J. Hazard. Mater. 178 (2010) 209–217.
[8] A.H. Malik, Z.M. Khan, Q. Mahmood, S. Nasreen, Z.A. Bhatti, Perspectives of low cost arsenic remediation of drinking water in Pakistan and other countries, J. Hazard. Mater. 168 (2009) 1–12.
[9] Y. Yoon, Y. Hwang, M. Ji, B.H. Jeon, J.W. Kang, Ozone-membrane hybrid process for arsenic removal in iron containing water, Desalin. Water Treat. 31 (2011) 138–143.

[10] S. Xia, B. Dong, Q. Zhang, B. Xu, N. Gao, C. Causseranda, Study of arsenic removal by nanofiltration and its application in China, Desalination 204 (2007) 374–379.
[11] M. Cakmakci, A.B. Baspinar, U. Balaban, V. Uyak, I. Koyuncu, C. Kinaci, Comparison of nanofiltration and adsorption techniques to remove arsenic from drinking water, Desalin. Water Treat. 9 (2009) 149–154.
[12] B. Zhao, H. Zhao, J. Ni, Arsenate removal by Donnan dialysis: Effects of the accompanying components, Sep. Purif. Technol. 72 (2010) 250–255.
[13] D. van Halem, S.G.J. Heijman, R. Johnston, I.M. Huq, S.K. Ghosh, J.Q.J.C. Verberk, G.L. Amy, J.C. Van Dijk, Subsurface iron and arsenic removal: Low-cost technology for community-based water supply in Bangladesh, Water Sci. Technol. 62 (2010) 2702–2709.
[14] G.S. Zhang, J.H. Qu, H.J. Liu, R.P. Liu, G.T. Li, Removal mechanism of As(III) by a novel Fe–Mn binary oxide adsorbent: Oxidation and sorption, Environ. Sci. Technol. 41 (2007) 4613–4619.
[15] D. Mohan, C.U. Pittman, Jr., Arsenic removal from water/wastewater using adsorbents—a critical review, J. Hazard. Mater. 142 (2007) 1–53.
[16] Y. Kim, C. Kim, I. Choi, S. Rengaraj, J. Yi, Arsenic removal using mesoporous alumina prepared via a templating method, Environ. Sci. Technol. 38 (2004) 924–931.
[17] H. Sun, X. Zhang, Z. Zhang, Y. Chen, J.C. Crittenden, Influence of titanium dioxide nanoparticles on speciation and bioavailability of arsenite, Environ. Pollut. 157 (2009) 1165–1170.
[18] Z. Xu, Q. Li, S. Gao, J.K. Shang, As(III) removal by hydrous titanium dioxide prepared from one-step hydrolysis of aqueous $TiCl_4$ solution, Water Res. 44 (2010) 5713–5721.
[19] L.K. Adams, D.Y. Lyon, P.J. Alvarez, Comparative eco-toxicity of nanoscale TiO_2, SiO_2, and ZnO water suspensions, Water Res. 40 (2006) 3527–3532.
[20] F.S. Zhang, H. Itoh, Photocatalytic oxidation and removal of arsenite from water using slag-iron oxide-TiO_2 adsorbent, Chemosphere 65 (2006) 125–131.
[21] M.E. Pena, G.P. Korfiatis, M. Patel, L. Lippincott, X. Meng, Adsorption of As(V) and As(III) by nanocrystalline titaniumdioxide, Water Res. 39 (2005) 2327–2337.
[22] S. Bang, M. Patel, L. Lippincott, X. Meng, Removal of arsenic from groundwater by granular titanium dioxide adsorbent, Chemosphere 60 (2005) 389–397.
[23] D. Nabi, I. Aslam, I.A. Qazi, Evaluation of the adsorption potential of titanium dioxide nanoparticles for arsenic removal, J. Environ. Sci. 21 (2009) 402–408.
[24] S. Dixit, J.G. Hering, Comparison of arsenic(V) and arsenic (III) sorption onto iron oxide minerals: Implications for arsenic mobility, Environ. Sci. Technol. 37 (2003) 4182–4189.
[25] G. Jegadeesan, S.R. Al-Abed, V. Sundaram, H. Choi, K.G. Scheckel, D.D. Dionysiou, Arsenic sorption on TiO_2 nanoparticles: Size and crystallinity effects, Water Res. 44 (2010) 965–973.
[26] B. Manna, M. Dasgupta, U.C. Ghosh, Crystalline hydrous titanium (IV) oxide (CHTO): An arsenic (III) scavenger from natural water, J. Water SRT—Aqua. 53 (2004) 483–495.
[27] X.H. Huang, Y.C. Tang, C. Hu, H.Q. Yu, C.S. Chen, Preparation and characterization of visible-light-active nitrogen-doped TiO_2 photocatalyst, J. Environ. Sci. 17 (2005) 562–565.
[28] National Environmental Protection Agency of China, Shui he feishui jiance fenxi fangfa [Analytical Methods for Water and Wastewater], Chinese Environmental Sciences Publishing Company, Beijing, 2002, pp. 306 (in Chinese).
[29] P.K. Dutta, A.K. Ray, V.K. Sharma, F.J. Millero, Adsorption of arsenate and arsenite on titanium dioxide suspensions, J. Colloid Interf. Sci. 278 (2004) 270–275.
[30] S. Kondo, T. Ishi Kawa, I. Abu, Adsorption Science, Trans. G. X. Li, second ed., Chemical Industry Press, Beijing, 2006, pp. 105 (in Chinese).
[31] K. Banerjee, G.L. Amy, M. Prevost, S. Nour, M. Jekel, P.M. Gallagher, C.D. Blumenschein, Kinetic and thermodynamic aspects of adsorption of arsenic onto granular ferric hydroxide (GFH), Water Res. 42 (2008) 3371–3378.
[32] J. Zhang, S. Robert, Slow adsorption reaction between arsenic species and goethite (a-FeOOH): Diffusion or heterogeneous surface reaction control, Langmuir 21 (2005) 2895–2901.
[33] D.L. Sparks, Soil Physical Chemistry, second ed., CRC Press, Boca Raton, FL, 1999.
[34] S. Kundu, A.K. Gupta, Adsorption characteristic of As(III) from aqueous solution on iron oxide coated cement (IOCC), J. Hazard. Mater. 142 (2007) 97–104.
[35] Y.N. Chen, L.Y. Chai, Y.D. Shu, Study of arsenic(V) adsorption on bone char from aqueous solution, J. Hazard. Mater. 160 (2008) 168–172.
[36] T.S. Singh, K.K. Pant, Equilibrium, kinetics and thermodynamic studies for adsorption of As(III) on activated alumina, Sep. Purif. Technol. 36 (2004) 139–147.
[37] S.K. Maji, A. Pal, T. Pal, Arsenic removal from real-life groundwater by adsorption on laterite soil, J. Hazard. Mater. 151 (2008) 811–820.
[38] G.N. Manju, C. Raji, T.S. Anirudhan, Evaluation of coconut husk carbon for the removal of arsenic from water, Water Res. 32 (1998) 3062–3070.
[39] V. Pallier, G. Feuillade-Cathalifaud, B. Serpaud, J.C. Bollinger, Effect of organic matter on arsenic removal during coagulation/flocculation treatment, J. Colloid Interf. Sci. 342 (2010) 26–32.
[40] H. Yang, W.Y. Lin, K. Rajeshwar, Homogeneous and teterogeneous photocatalytic reactions involving As(III) and As(V) species in aqueous media, J. Photochem. Photobiol. A 123 (1999) 137–143.
[41] H. Guo, D. Stüben, Z. Berner, Adsorption of arsenic(III) and arsenic(V) from groundwater using natural siderite as the adsorbent, J. Colloid Interf. Sci. 315 (2007) 47–53.
[42] S. Kundu, A.K. Gupta, Adsorptive removal of As(III) from aqueous solution using iron oxide coated cement (IOCC): Evaluation of kinetic, equilibrium and thermodynamic models, Sep. Purif. Technol. 51 (2006) 165–172.
[43] O.S. Thirunavukkarasu, T. Viraraghavan, K.S. Subramanian, O. Chaalal, M.R. Islam, Arsenic removal in drinking water-impacts and novel removal technologies, Energy Sour. 27 (2005) 209–219.
[44] J.C. Hsu, C.J. Lin, C.H. Liao, S.T. Chen, Removal of As(V) and As(III) by reclaimed iron-oxide coated sands, J. Hazard. Mater. 153 (2008) 817–826.
[45] M.S. Rahaman, A. Basu, M.R. Islam, The removal of As(III) and As(V) from aqueous solutions by waste materials, Bioresour. Technol. 99 (2008) 2815–2823.
[46] S.R. Kanel, B. Manning, L. Charlet, H. Choi, Removal of arsenic(III) from groundwater by nanoscale zero-valent iron, Environ. Sci. Technol. 39 (2005) 1291–1298.